

Mechanism of Ultraviolet-Induced CO Desorption from CO Ice: Role of Vibrational Relaxation Highlighted

Samuel Del Fré^{1,*}, Alejandro Rivero Santamaría^{1,†}, Denis Duflot^{1,‡}, Romain Basalgèze^{2,§}, Géraldine Féraud^{2,||},
Mathieu Bertin^{2,¶}, Jean-Hugues Fillion^{2,**} and Maurice Monnerville^{1,††}

¹Univ. Lille, CNRS, UMR 8523 - PhLAM - Physique des Lasers Atomes et Molécules, F-59000 Lille, France

²Sorbonne Université, Observatoire de Paris, Université PSL, CNRS, LERMA, F-75005 Paris, France



(Received 23 May 2023; accepted 13 October 2023; published 6 December 2023)

Although UV photon-induced CO ice desorption is clearly observed in many cold regions of the Universe as well as in the laboratory, the fundamental question of the mechanisms involved at the molecular scale remains debated. In particular, the exact nature of the involved energy transfers in the indirect desorption pathway highlighted in previous experiments is not explained. Using *ab initio* molecular dynamics simulations, we explore a new indirect desorption mechanism in which a highly vibrationally excited CO ($v = 40$) within an aggregate of 50 CO molecules triggers the desorption of molecules at the surface. The desorption originates first from a mutual attraction between the excited molecule and the surrounding molecule(s), followed by a cascade of energy transfers, ultimately resulting in the desorption of vibrationally cold CO ($\sim 95\%$ in $v = 0$). The theoretical vibrational distribution, along with the kinetic energy one, which peaks around 25 meV for CO with low rotational levels ($v = 0, J < 7$), is in excellent agreement with the results obtained from VUV laser induced desorption (157 nm) of CO ($v = 0, 1$) probed using REMPI.

DOI: [10.1103/PhysRevLett.131.238001](https://doi.org/10.1103/PhysRevLett.131.238001)

Carbon monoxide (CO) is known to be a primordial tracer of the gas phase density and temperature of many regions of the interstellar medium (ISM). In star and planet-forming cold regions, gaseous CO undergoes a freeze-out onto (sub)micron-sized dust grains, resulting in the formation of solid CO layers [1,2]. This condensation is, however, counterbalanced by nonthermal desorption processes, maintaining a certain budget of rotationally cold carbon monoxide into the gas phase (e.g., [3]). The desorption subsequent to the irradiation of the icy grains by vacuum UV (VUV) photons (5–13.6 eV), has been for a long time proposed as a dominant mechanism, for instance, in protoplanetary disks [4]. Constraining the efficiency and mechanisms of the CO UV-photodesorption became of paramount importance since it may impact both the location of the CO snowlines, thereby affecting the formation dynamics and composition of exoplanets [5–7], and the chemical richness in these cold media as CO ices are a potential starting point for a complex chemistry leading to methanol formation, and to a rich subsequent organic chemistry [8,9]. For these reasons, the VUV-photodesorption of solid CO has been for decades the subject of a large panel of experimental studies aiming to provide absolute desorption yields to the astrochemical community [10–17]. Below 10 eV, the yield is of about 1 desorbed molecule per absorbed photon, although it depends on the temperature at which the ice was grown [15]. The desorption has been shown to be triggered by the $A^1\Pi - X^1\Sigma^+$ transition in the 7–10 eV energy range [desorption induced by electronic

transition (DIET) mechanism [13]] and to involve the 2 to 5 outmost layers of the ice only (~ 7 to 18 Å) [12,14,18]. The exact mechanism at the origin of the desorption is, however, still largely unknown and its dependence on many parameters is still debated. Probably the most striking property of the mechanism is that it is mostly indirect: synchrotron-based experiments have revealed that the desorbing molecule is not necessarily the one which absorbed the photon, but instead the dominating process involves an energy transfer between the excited molecule and a surface molecule [14]. This indirect desorption has even been shown to be operative between an excited CO and other coadsorbed molecules, such as N₂ or CH₄ [18,19], making this mechanism particularly interesting to predict photodesorption yields from composite, and thus more astrophysically relevant, ices. However, none of the above-mentioned experimental studies were able to propose a detailed desorption mechanism that would explain all the observed properties, and, in particular, none could bring a hint on the exact nature of the involved energy transfer, mainly because none could access the total energy balance of the process by probing the amount of translational and internal energy left in the desorbates. There is only one detailed theoretical study concerning the photodesorption of pure CO ices performed by van Hemert *et al.* [20]. They simulated the dynamics of large amorphous and crystalline CO clusters after the UV excitation of a single CO molecule by using molecular dynamics (MD) simulations based on a classical force field. The proposed

mechanism involves the excited molecule which, after internal conversion, lands back to its fundamental electronic state in a very high vibrational state, thus leading to its direct desorption or to an indirect desorption of a neighboring molecule. Their simulation estimates the probability of photodesorption to be a factor of 3 to 11 lower than the experimental one [13], and the indirect pathway is rather minor compared to the direct one. This is in contradiction with the experimental results described above. In addition, their model also predicts an absence of desorption when a CO molecule is directly vibrationally excited in its electronic ground state.

Here, we make a new proposition for the microscopic mechanism involved in the solid CO photodesorption, with the specific aim to finally characterize the indirect desorption and the nature of the energy transfer between the excited molecule and its neighbors. The methodology we employ is based on a coupled experimental and theoretical strategy. New VUV photodesorption experiments, that provide vibrational and translational energy distribution of the photodesorbed CO molecules, are performed. The obtained results are compared with *ab initio* molecular dynamics (AIMD) simulations performed with the Vienna *ab initio* simulation package (VASP) based on density functional theory (DFT) [21,22]. For these calculations we use the Perdew-Burke-Ernzerhof (PBE) [23] exchange-correlation functional, together with the DFT-D3(BJ) dispersion correction [24,25].

The experiments were performed using an ultrahigh vacuum setup (base pressure of $\sim 10^{-10}$ Torr). A pure CO ice (~ 100 ML) was deposited onto a polycrystalline oxygen-free high-conductivity copper substrate cooled down at 15 K by a closed-cycle Helium cryostat. VUV photons were generated by four-wave frequency mixing in Xe [26,27], resulting in a pulsed VUV beam (10 Hz, duration of 10 ns, 10^6 photons per pulse) that was tuned to the A-X (0,0) transition of CO (157 nm) and focused at the CO ice. The individual rovibrational states of photodesorbed neutral CO (v, J) were probed by a resonance-enhanced multi-photon ionization (REMPI) technique using a tunable pulsed laser (OPO, 200–700 nm) focused a few millimeters in front of the ice surface. After resonant ionization of ${}^1\Sigma^+$ CO (v, J) states, the ions are detected by mass spectrometry using a quadrupole mass spectrometer equipped with an ion extractor. The Q branches of the REMPI($2 + 1$) $B^1\Sigma^+(v' = 0 \text{ or } 1) \leftarrow X^1\Sigma^+(v'' = 0 \text{ or } 1)$ bands near 230 nm [28] were used to probe the distribution of rovibrational states populated after desorption. The search for vibrationally excited CO in the $v = 2$ (near 230.5 nm), 16 (near 224.9 nm), and 19 (near 246.4 nm) states was also carried out, but no ionization signal was found. The kinetic energy distribution of photodesorbing CO molecules was estimated by monitoring the variations of the ion signal with the time delay between the VUV pulse (desorption event) and the ionizing pulse (probe

event), referred to as the time-of-flight (TOF) of the photodesorbing molecules. TOF spectra are then converted to give one kinetic energy distribution following the Zimmermann *et al.* approach [29]. More details about the experimental technique can be found in the Supplemental Material [30], and in [57].

The AIMD simulations focused on the description of the vibrational energy redistribution when an excited CO molecule transfers its electronic energy to a high vibrational state of its ground state. This phase corresponds to the part of the DIET mechanism after the internal conversion. Particularly, the first three bands $A^1\Pi(v' = 0, 1, 2) \leftarrow X^1\Sigma^+(v'' = 0)$ of the absorption spectrum correspond to an internal energy ranging between 8 and 8.4 eV, which can promote the molecule to the electronic ground vibrational levels $v = 39\text{--}41$. Aggregates of 50 CO molecules were generated, optimized, and finally thermalized (15 K) using canonical AIMD calculations. The aggregate phase space configurations obtained after the thermalization process were modified to vibrationally excite a single CO molecule ($v = 40$ in this work) located in the central core of the aggregate (further details in [30]). Following a standard procedure in gas-surface dynamics simulations [37–45] a random aggregate prepared as mentioned above, was selected for each trajectory to run constant energy AIMD calculations. Finally, under these conditions, 100 AIMD trajectories were propagated using VASP. The maximum propagation time was 5 ps with a time step of 0.5 fs. Two possible exit channels were taken into account, called desorption and nondesorption: a molecule was considered desorbed when the distance from the CO center of mass and the aggregate surface exceeded 3 Å and not desorbed when after 5 ps no molecule fulfilled the above condition. The total energy was well conserved for each trajectory with a standard deviation of ~ 30 meV. The energy distributions of the molecules along the dynamics were obtained using the standard semiclassical determination method for the translational, vibrational, and rotational energies [58].

Among the 100 trajectories, 88% resulted in the desorption of CO molecule(s). The average desorption time was 2 ps and interestingly, the desorption was not observed before 700 fs, suggesting that more complex mechanisms than a fast release of the excited molecules into the gas phase must take place. An example of the time evolution of a typical trajectory for which desorption takes place is presented in Fig. 1. By closely examining this trajectory we can conclude that the dynamics of the desorption process can be described in three fundamental steps: (1) First, the excited molecule vibrates inside the aggregate while retaining the initially deposited vibrational energy. No significant energy transfers to other modes (translational or rotational) are observed. (2) The excited molecule and one ($\sim 75\%$) or two ($\sim 25\%$) CO molecule(s) in its vicinity begin to be mutually attracted and accordingly gain translational energy, thus leading to their collision via a “kick

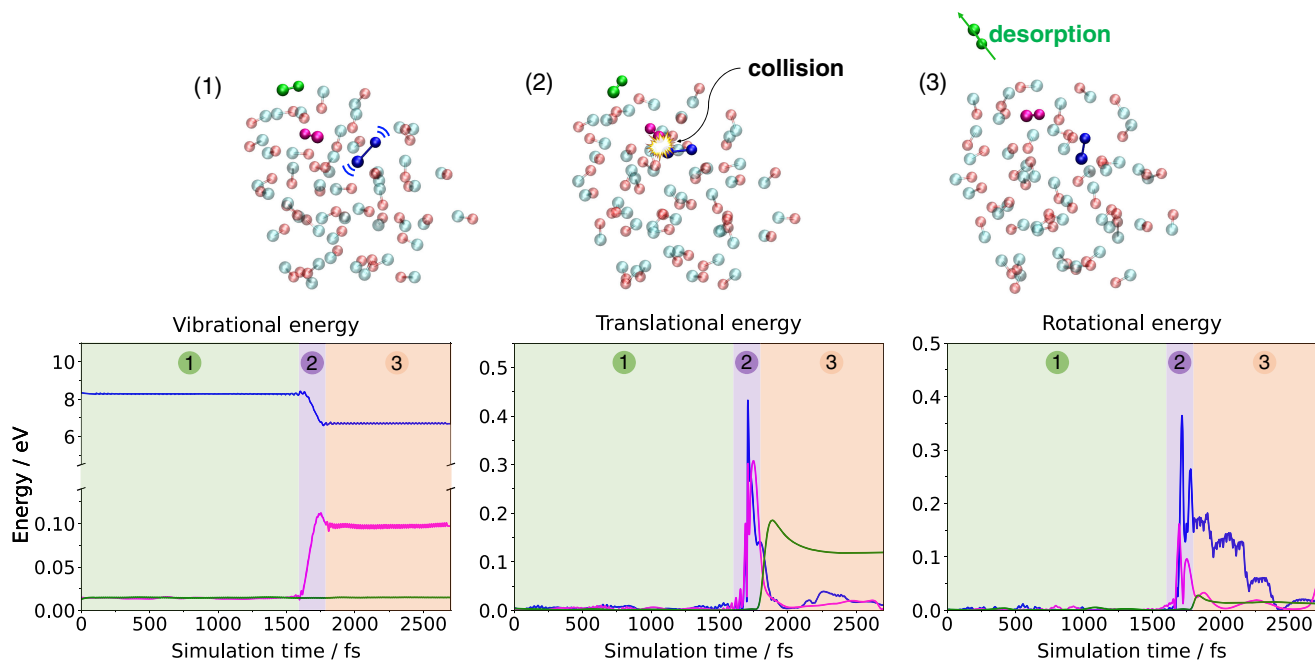


FIG. 1. Upper panel: Snapshots of a typical desorbing trajectory. The excited (blue), kicked (magenta), and desorbed (green) molecules are highlighted. Lower panel: Vibrational, translational, and rotational energy of the excited, kicked, and desorbed CO molecules along the trajectory depicted in the upper panel. The numbers 1 to 3 refer to the three fundamental steps of the desorption process.

event.” At this time, sudden intra- and intermolecular energy transfers from the vibration to the translational, rotational, and vibrational modes of the colliding molecules occur. (3) The colliding molecules begin to move and interact with other molecules within the aggregate leading to a cascade energy transfer effect; i.e., the translational and rotational energy acquired in step 2 is transferred to surface CO molecule(s) thus giving it (them) enough kinetic energy to exceed the binding energy of the aggregate (around 100 meV in our case).

The analysis of a typical trajectory where no desorption is observed (see Fig. S2 in [30]) shows that a smaller fraction of the vibrational energy of the excited molecule is transferred to the other energy modes during the kick, in contrast to events where desorption occurs. The amount of translational energy gained by the colliding molecules is not sufficient to observe the cascade energy transfer effect explained above. Therefore, the kick event plays a fundamental role to achieve sufficient energy transfers and to observe desorption.

To further investigate the colliding molecules kick event, we present in Fig. 2 some interaction energy curves between two CO molecules (*A* and *B*). The curves were obtained under the previously described computational conditions by fixing the bond lengths of *A* to its equilibrium geometry ($r_A = 1.14$ Å) and *B* to the calculated outer turning point of the vibrational state $v = 40$ ($r_B = 1.98$ Å). The two molecules were then placed in the *xy*

plane with the two C facing each other in a displaced-stacked manner at fixed distances of 0.5, 1.5, 2.0, and 2.5 Å between the two molecules’ centers of mass in the *y* direction (see Fig. 2). These particular geometries aim to mimic the disposition of the colliding molecules in the aggregate. The interaction energy $E_{AB} = E_{\text{tot}} - E_A - E_B$ between molecules *A* and *B* was then scanned while approaching them along the *x* axis. The results show that there exists an attractive potential energy well between the two molecules which is not observed for configurations

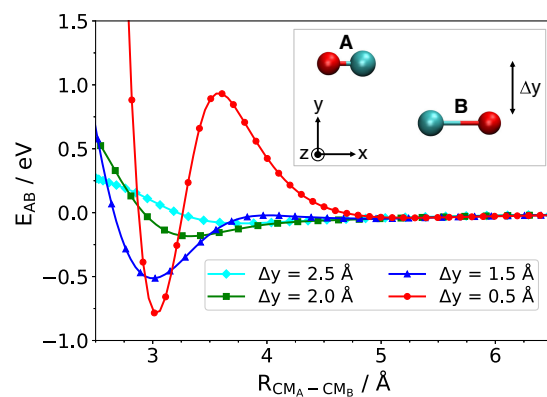


FIG. 2. Interaction energy evolution between two CO molecules (*A* and *B*) as a function of the distance between their centers of mass for fixed Δy values. The CO molecules bond lengths are set to $r_A = 1.14$ and $r_B = 1.98$ Å.

where the two molecules are taken at the equilibrium bond length $r_A = r_B = 1.14 \text{ \AA}$ (see Fig. S3 in [30]). In general, starting from geometries where the molecules are far apart ($\Delta y = 2.5 \text{ \AA}$) to those where they are closer ($\Delta y = 0.5 \text{ \AA}$), the position of the well shifts towards smaller distances and its depth increases. In particular, the closest conformation to the kick event geometry (red curve, at distance around 3 \AA in Fig. 2) exhibits the strongest interaction ($E_{AB} \sim -0.8 \text{ eV}$). The existence of such attraction is likely explained by the particular evolution of the CO dipole moment upon bond stretching in the r_{CO} range explored in our simulations. As has been previously shown (e.g., [54,59–62]), the CO displays a dipole moment of $\sim 0.12 \text{ D}$ [62] in the direction $C^{\delta-}O^{\delta+}$ at equilibrium, but it reverses to $C^{\delta+}O^{\delta-}$ and increases at larger r_{CO} up to its maximum value of $\sim 1.45 \text{ D}$ for $r_{CO} \sim 1.95 \text{ \AA}$ [62]. Hence, a highly attractive dipole-dipole interaction is created between two CO molecules when one of them starts to vibrate, especially at high v . It should be mentioned that a similar electrostatic behavior when the CO stretch is excited has already been highlighted in several studies on the CO-NaCl system, e.g., [63–65].

The agreement between past experiments, notably [14], and theory is remarkable since in both cases, the large majority of UV excitations (experiments) or vibrational excitations (simulations) of CO molecules results in a desorption event. The high probability, observed in our simulations, in the indirect desorption channel is in disagreement with the results of van Hemert *et al.* [20] that show a very small contribution of the indirect pathway. However, in order to directly compare these results with our calculations, it is necessary to note that our study was focused on the second part of the DIET mechanism, so it did not take into account the configuration space explored by the molecule in the excited electronic state potential energy surface (PES) after the UV excitation. Nonetheless, our simulation provides very valuable information about the mechanism of vibrational deexcitation of the CO molecule within the aggregate. Indeed, our results clearly indicate that the transfer from vibrational to translational energy modes inside the CO aggregates is essential in the desorption mechanism. The significant discrepancy regarding the role of vibrational energy transfer between our theoretical results and those obtained by van Hemert *et al.* [20], could be related to the different methods used to describe the interactions in the simulations. The analytical PESs used in [20] (ground and excited states) are pairwise potentials based on CO dimers interaction. The site-site PES, frequently used to study this kind of system, may, however, present difficulties to describe the multibody effects in complex systems. Our results indicate that the discrepancies primarily stem from the limited sampling of their analytical ground state PES, which only includes the first three vibrational levels of the CO ground state. The lack of points describing higher vibrational levels seems to

be the cause of the difficulties for the mentioned PES to correctly describe the interactions between a highly vibrationally excited CO molecule with its pair at the equilibrium bond length. This is confirmed by the interaction energy curves (see Fig. S4 in [30]) obtained using the aforementioned PES that do not correctly describe the attractive potential energy well observed in our calculations (see Fig. 2), which is responsible for triggering the collision between the excited CO molecule and the surrounding CO molecule(s).

Finally, the remarkable quantitative and qualitative agreement between our simulations and experiments is confirmed by comparing the vibrational and kinetic energy distributions of the desorbed molecules. Experimentally, the photodesorbed CO molecules were found to be mostly in their ground vibrational level ($\sim 96\%$ in the $v = 0$ level) while the population of the $v = 1$ level is estimated to $\sim 4\%$. It should be mentioned that the chosen REMPI transition (near 230 nm) allows only to detect vibrationally cold CO ($v = 0, 1$). However, our simulations show also that the desorbed molecules are predominantly vibrationally cold ($\sim 95\%$ of $v = 0$) and desorption of molecules with $v > 0$ is observed only in the rare cases where the excited molecule kicked a molecule close to the surface, resulting in desorption of the latter. Figure 3 shows the experimental (derived from TOF spectra, see Fig. S5 in [30]) and theoretical translational energy distributions of the desorbed molecules in the $v = 0$ and $J < 7$ states. A non-Boltzmann kinetic energy distribution has been observed in both cases, with the maximum of the distributions located around 25 meV , and very few molecules were detected with translational energies higher than 200 meV . Therefore, only a small fraction ($\sim 2\%$) of the vibrational energy initially deposited is finally transferred to the desorbed molecule(s). In fact, even if the initial vibrational energy dissipates within the aggregate in its different modes, only a minimum translational energy is

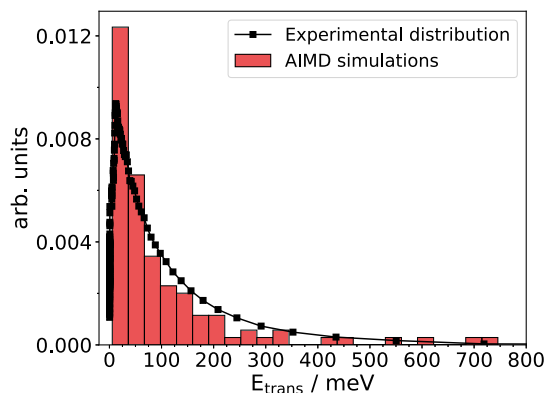


FIG. 3. Experimental kinetic energy distribution derived from the TOF spectra [30] (black curve) and theoretical kinetic energy distribution of the desorbed CO molecules (red bars).

required to separate a molecule from the aggregate. This minimum energy is acquired by the future desorbed molecule(s) through a final collision. In particular, our simulations show that this type of event transmits between 100 and 300 meV to the molecule(s) translational mode. This kinetic energy is mainly used to overcome the desorption barrier (~ 100 meV) and the remaining energy (between ~ 5 – 200 meV) is used by the molecule(s) to move away from the aggregate.

In summary, we performed both experiments on UV photodesorption from CO amorphous ice and AIMD simulations on the vibrational excitation ($v = 40$) of one CO within an aggregate of 50 CO molecules. A detailed analysis of the energy transfers taking place in the aggregate was conducted in the simulations to explain the desorption mechanism. We have shed new light on the UV-induced photodesorption mechanism of CO from pure CO ice by highlighting the essential role of molecular vibration in triggering desorption. In particular, the theoretical analysis of the energy redistribution after the vibrational excitation shows that sufficient energy transfers between the excited molecule and neighboring one(s) occur, leading to the indirect desorption of CO molecule (s) in almost all trajectories after a kick event. We have shown that this kick can be explained by a strong attractive interaction created between two CO molecules when one of them starts to vibrate. Finally, the vibrational and kinetic energy characteristics of the desorbed molecules obtained from the experiments and the simulations have been found to be remarkably consistent, thus providing substantial support to the fundamental role of vibrational deexcitation in the desorption mechanism. The methodology implemented here is easily applicable to more complex ice mixtures, more relevant to their field of study. Indeed, the fate of the energy transfers, potentially leading to indirect desorption, when an electronically excited CO molecule is surrounded by other diatomic (e.g., N_2 , O_2 , NO) or larger (e.g. CH_3OH) molecules is a fundamental question of high interest for several fields (e.g., astrophysics, terrestrial atmosphere).

This project was provided with computer and storage resources by GENCI at TGCC thanks to the grants 2022-A0110801859 and 2023-A0130801859 and by the Centre de Ressources Informatiques (CRI) of the Université de Lille. This work was funded by the ANR PIXyES project, Grant ANR-20-CE30-0018 of the French Agence Nationale de la Recherche, by the Region Ile-de-France DIM-ACAV+ program, and by the French Programme National “Physique et Chimie du Milieu Interstellaire” (PCMI) of CNRS/INSU cofunded by CEA and CNES. We also acknowledge funding from Labex MiChem, part of the French state funds managed by the ANR within the investissements d’avenir program under Reference No. ANR-11-10EX-0004-02, and from the INSU-CSAA.

*samuel.del-fre@univ-lille.fr

†alejandro.rivero@univ-lille.fr

‡denis.duflot@univ-lille.fr

§romain.basalgete@sorbonne-universite.fr

||geraldine.feraud@sorbonne-universite.fr

¶mathieu.bertin@sorbonne-universite.fr

**jean-hugues.fillion@sorbonne-universite.fr

††maurice.monnerville@univ-lille.fr

- [1] K. M. Pontoppidan, H. J. Fraser, E. Dartois, W. F. Thi, E. F. van Dishoeck, A. C. A. Boogert, L. d’Hendecourt, A. Tielens, and S. E. Bisschop, *Astron. Astrophys.* **408**, 981 (2003).
- [2] A. A. Boogert, P. A. Gerakines, and D. C. Whittet, *Annu. Rev. Astron. Astrophys.* **53**, 541 (2015).
- [3] V. Piétu, A. Dutrey, and S. Guilloteau, *Astron. Astrophys.* **467**, 163 (2007).
- [4] K. Willacy and W. D. Langer, *Astrophys. J.* **544**, 903 (2000).
- [5] K. I. Öberg, R. Murray-Clay, and E. A. Bergin, *Astrophys. J. Lett.* **743**, L16 (2011).
- [6] K. I. Öberg and E. A. Bergin, *Phys. Rep.* **893**, 1 (2021).
- [7] M. Minissale, Y. Aikawa, E. Bergin, M. Bertin, W. A. Brown, S. Cazaux, S. B. Charnley, A. Coutens, H. M. Cuppen, V. Guzman, H. Linnartz, M. R. S. McCoustra, A. Rimola, J. G. Schrauwen, C. Toubin, P. Ugliengo, N. Watanabe, V. Wakelam, and F. Dulieu, *ACS Earth Space Chem.* **6**, 597 (2022).
- [8] N. Watanabe and A. Kouchi, *Astrophys. J. Lett.* **571**, L173 (2002).
- [9] G. W. Fuchs, H. M. Cuppen, S. Ioppolo, C. Romanzin, S. E. Bisschop, S. Andersson, E. F. van Dishoeck, and H. Linnartz, *Astron. Astrophys.* **505**, 629 (2009).
- [10] K. I. Öberg, G. W. Fuchs, Z. Awad, H. J. Fraser, S. Schlemmer, E. F. Van Dishoeck, and H. Linnartz, *Astrophys. J.* **662**, L23 (2007).
- [11] K. I. Öberg, E. F. van Dishoeck, and H. Linnartz, *Astron. Astrophys.* **496**, 281 (2009).
- [12] G. M. Muñoz Caro, A. Jimenez-Escobar, J. A. Martin-Gago, C. Rogero, C. Atienza, S. Puertas, J. M. Sobrado, and J. Torres-Redondo, *Astron. Astrophys.* **522**, A108 (2010).
- [13] E. C. Fayolle, M. Bertin, C. Romanzin, X. Michaut, K. I. Öberg, H. Linnartz, and J.-H. Fillion, *Astrophys. J. Lett.* **739**, L36 (2011).
- [14] M. Bertin, E. C. Fayolle, C. Romanzin, K. I. Öberg, X. Michaut, A. Moudens, L. Philippe, P. Jeseck, H. Linnartz, and J.-H. Fillion, *Phys. Chem. Chem. Phys.* **14**, 9929 (2012).
- [15] G. M. Muñoz Caro, Y.-J. Chen, S. Aparicio, A. Jiménez-Escobar, A. Rosu-Finsen, J. Lasne, and M. R. S. McCoustra, *Astron. Astrophys.* **589**, A19 (2016).
- [16] D. M. Paardekooper, G. Fedoseev, A. Riedo, and H. Linnartz, *Astron. Astrophys.* **596**, A72 (2016).
- [17] N.-E. Sie, Y.-T. Cho, C.-H. Huang, G. M. M. Caro, L.-C. Hsiao, H.-C. Lin, and Y.-J. Chen, *Astrophys. J.* **938**, 48 (2022).
- [18] M. Bertin, E. C. Fayolle, C. Romanzin, H. A. M. Poderoso, X. Michaut, L. Philippe, P. Jeseck, K. I. Öberg, H. Linnartz, and J.-H. Fillion, *Astrophys. J.* **779**, 120 (2013).
- [19] R. Dupuy, M. Bertin, G. Féraud, X. Michaut, P. Jeseck, M. Doronin, L. Philippe, C. Romanzin, and J.-H. Fillion, *Astron. Astrophys.* **603**, A61 (2017).

- [20] M. C. van Hemert, J. Takahashi, and E. F. van Dishoeck, *J. Phys. Chem. A* **119**, 6354 (2015).
- [21] G. Kresse and J. Furthmüller, *Comput. Mater. Sci.* **6**, 15 (1996).
- [22] G. Kresse and J. Furthmüller, *Phys. Rev. B* **54**, 11169 (1996).
- [23] J. P. Perdew, K. Burke, and M. Ernzerhof, *Phys. Rev. Lett.* **77**, 3865 (1996).
- [24] S. Grimme, J. Antony, S. Ehrlich, and H. Krieg, *J. Chem. Phys.* **132**, 154104 (2010).
- [25] S. Grimme, S. Ehrlich, and L. Goerigk, *J. Comput. Chem.* **32**, 1456 (2011).
- [26] R. Hilbig and R. Wallenstein, *Appl. Opt.* **21**, 913 (1982).
- [27] R. Hilbig and R. Wallenstein, *IEEE J. Quantum Electron.* **19**, 194 (1983).
- [28] S. Wurm, P. Feulner, and D. Menzel, *J. Chem. Phys.* **105**, 6673 (1996).
- [29] F. M. Zimmermann and W. Ho, *Surf. Sci. Rep.* **22**, 127 (1995).
- [30] See Supplemental Material at <http://link.aps.org/supplemental/10.1103/PhysRevLett.131.238001> for computational and experimental details, which includes Refs. [20–29,31–56].
- [31] P. E. Blöchl, *Phys. Rev. B* **50**, 17953 (1994).
- [32] G. Kresse and D. Joubert, *Phys. Rev. B* **59**, 1758 (1999).
- [33] H. J. Monkhorst and J. D. Pack, *Phys. Rev. B* **13**, 5188 (1976).
- [34] A. Cassidy, M. R. S. McCoustra, and D. Field, *Acc. Chem. Res.* **56**, 1909 (2023).
- [35] S. Nosé, *J. Chem. Phys.* **81**, 511 (1984).
- [36] W. G. Hoover, *Phys. Rev. A* **31**, 1695 (1985).
- [37] A. Groß and A. Dianat, *Phys. Rev. Lett.* **98**, 206107 (2007).
- [38] F. Nattino, C. Díaz, B. Jackson, and G.-J. Kroes, *Phys. Rev. Lett.* **108**, 236104 (2012).
- [39] F. Nattino, H. Ueta, H. Chadwick, M. E. van Reijzen, R. D. Beck, B. Jackson, M. C. van Hemert, and G.-J. Kroes, *J. Phys. Chem. Lett.* **5**, 1294 (2014).
- [40] B. Kolb and H. Guo, *J. Chem. Phys.* **145**, 011102 (2016).
- [41] D. Novko, I. Lončarić, M. Blanco-Rey, J. I. Juaristi, and M. Alducin, *Phys. Rev. B* **96**, 085437 (2017).
- [42] X. Zhou, B. Kolb, X. Luo, H. Guo, and B. Jiang, *J. Phys. Chem. C* **121**, 5594 (2017).
- [43] L. Zhou, B. Jiang, M. Alducin, and H. Guo, *J. Chem. Phys.* **149**, 031101 (2018).
- [44] G. Fuchsels, X. Zhou, B. Jiang, J. I. Juaristi, M. Alducin, H. Guo, and G.-J. Kroes, *J. Phys. Chem. C* **123**, 2287 (2019).
- [45] A. Rivero Santamaría, M. Alducin, R. Diez Muiño, and J. I. Juaristi, *J. Phys. Chem. C* **123**, 31094 (2019).
- [46] H.-J. Werner and P. J. Knowles, *J. Chem. Phys.* **89**, 5803 (1988).
- [47] P. J. Knowles and H.-J. Werner, *Chem. Phys. Lett.* **145**, 514 (1988).
- [48] S. R. Langhoff and E. R. Davidson, *Int. J. Quantum Chem.* **8**, 61 (1974).
- [49] H.-J. Werner and P. J. Knowles, *J. Chem. Phys.* **82**, 5053 (1985).
- [50] P. J. Knowles and H.-J. Werner, *Chem. Phys. Lett.* **115**, 259 (1985).
- [51] T. V. Mourik, A. K. Wilson, and T. H. Dunning, *Mol. Phys.* **96**, 529 (1999).
- [52] A. K. Wilson, T. van Mourik, and T. H. Dunning, *J. Mol. Struct.* **388**, 339 (1996).
- [53] H.-J. Werner, P. J. Knowles, F. R. Manby, J. A. Black, K. Doll, A. Heßelmann, D. Kats, A. Köhn, T. Korona, D. A. Kreplin, Q. Ma, T. F. Miller, A. Mitrushchenkov, K. A. Peterson, I. Polyak, G. Rauhut, and M. Sibae, *J. Chem. Phys.* **152**, 144107 (2020).
- [54] N. He, M. Huang, and F. A. Evangelista, *J. Phys. Chem. A* **127**, 1975 (2023).
- [55] A. A. Radzig and B. M. Smirnov, *Reference Data on Atoms, Molecules, and Ions* (Springer Science & Business Media, New York, 2012), Vol. 31.
- [56] S. Wurm, State-resolved investigation of the energy distribution over all degrees of freedom of electronically stimulated desorbed CO from monolayers, and condensates, Ph.D. thesis, Technische Universität München, 1995.
- [57] R. Basalgète, Laboratory Astrophysics applied to the VUV and X-ray photo-induced desorption from molecular ices, Ph.D. thesis, The institution is Sorbonne Université, 2022.
- [58] G. D. Billing, *Dynamics of Molecule Surface Interaction* (John Wiley & Sons, New York, 2000).
- [59] S. R. Langhoff and C. W. Bauschlicher Jr, *J. Chem. Phys.* **102**, 5220 (1995).
- [60] M. Buldakov, V. Cherepanov, E. Koryukina, and Y. N. Kalugina, *J. Phys. B* **42**, 105102 (2009).
- [61] J. Chen, J. Li, J. M. Bowman, and H. Guo, *J. Chem. Phys.* **153**, 054310 (2020).
- [62] V. V. Meshkov, A. Y. Ermilov, A. V. Stolyarov, E. S. Medvedev, V. G. Ushakov, and I. E. Gordon, *J. Quant. Spectrosc. Radiat. Transfer* **280**, 108090 (2022).
- [63] J. Chen, S. Hariharan, J. Meyer, and H. Guo, *J. Phys. Chem. C* **124**, 19146 (2020).
- [64] A. Nandi, P. Zhang, J. Chen, H. Guo, and J. M. Bowman, *Nat. Chem.* **13**, 249 (2021).
- [65] A. D. Boese and P. Saalfrank, *J. Phys. Chem. C* **120**, 12637 (2016).